Towards a mid-infrared *L* band up-conversion interferometer: first on-sky sensitivity test on a single arm

Lucien Lehmann [1]⋆ Ludovic Grossard,[1] Laurent Delage,[1] François Reynaud,[1] Mathieu Chauvet,[2] Florent Bassignot,[3] Frantz Martinache,[4] Frédéric Morand,[4] Jean-Pierre Rivet,[4] François-Xavier Schmider[4] and David Vernet[5]

[1]*Univ. Limoges, CNRS, XLIM, UMR 7252, F-87000 Limoges, France*
[2]*FEMTO-ST Institute, UMR CNRS 6174, Université de Bourgogne Franche-Comté, 25000 Besançon, France*
[3]*Femto-Engineering, 15B avenue des Montboucons, 25000 Besançon, France*
[4]*Université Côte d'Azur, Observatoire de la Côte d'Azur, CNRS, Laboratoire Lagrange, Bd de l'Observatoire, CS 34229, 06304 Nice cedex 4, France*
[5]*Université Côte d'Azur, Observatoire de la Côte d'Azur, CNRS, Dept. Galilée, Bd de l'Observatoire, CS 34229, 06304 Nice cedex 4, France*

ABSTRACT

We report on the first on-sky sensitivity test on a single arm of the Astronomical Light Optical Hybrid Analysis (ALOHA) instrument, an uncooled up-conversion interferometer in the *L* band (3.5 μm). Despite a low coupling efficiency (in the range of 1 per cent) between the 1-m class telescope and our instrument, we detect a magnitude $L_{mag} = 2.8$ star with a signal-to-noise ratio SNR = 2.7 over a 30 min integration time and with a spectral resolution $\lambda/\Delta\lambda = 100$. As the ALOHA project aims to shift light from the *L* band to the near-infrared, the use of very low loss silica optical fibres is an important step towards fibre-linked very long-baseline interferometry in the mid-infrared.

Key words: instrumentation: detectors – instrumentation: high angular resolution – techniques: interferometric.

1 INTRODUCTION

Interferometric instruments in astronomy measure the degree of coherence of the electric fields collected by an array of telescopes (Lawson 1997). The extension of this method to the mid-infrared (MIR) spectral domain (*L*, *M*, and *N* astronomical bands) offers great opportunities to investigate objects of primary interest such as active galactic nuclei, young stellar objects, and the formation or evolution of planetary systems. This was achieved with IOTA (Mennesson et al. 1999), and is one of the scientific goals of instruments like the LBTI (Hinz et al. 2016), the second-generation instrument MATISSE (Lopez et al. 2014) now operated on the Very Large Telescope Interferometer, and the interferometric nuller project Hi-5 (Defrère et al. 2018).

The sensitivity of instruments observing in this spectral domain is severely impacted by the thermal background induced by the instruments themselves. Mitigation of this background requires the implementation of cryogenic systems for the detector as well as the optical chain. The current lack of high-performance waveguides also prohibits the kilometric baselines that would be required by a concept like the Planet Formation Imager (Monnier et al. 2018).

An alternative architecture uses non-linear optics to frequency-shift the MIR light collected by the telescopes making up the interferometer, to the near-infrared (NIR) domain, while preserving the mutual coherence properties of the light. There are several advantages to this proposal. First, the converted light falls within the silica optical fibre transparency window. The use of single mode (SM) fibres enables efficient spatial filtering leading to much more stable fringe contrasts (Foresto 1994) and phase closure (Petrov et al. 2007) measurements and, hence, higher dynamic ranges. The coherent light transport through optical fibres can then be considered for very long baseline interferometer (Delage & Reynaud 2001) in the MIR wavelength domain. Secondly, the frequency shift strongly limits the effects of thermal background radiated by the different elements of the optical train (mirrors, windows, beam splitters...). Finally, the spectral shift allows us to efficiently use detectors working in the photon counting regime at room temperature. Fig. 1 presents a possible 2T-interferometer implementation of this concept called Astronomical Light Optical Hybrid Analysis (ALOHA) (Lehmann et al. 2018a).

After having demonstrated the possibility to detect on the sky interference fringes, using star light up-converted from the *H* band to the visible (up to $H_{mag} = 3.0$ with a spectral resolution equal to 2600), (Darré et al. 2016) at the Center for High Angular Resolution Astronomy (CHARA) Array (Brummelaar et al. 2005) and in the lab with a monochromatic coherent source at 3.39 μm (Szemendera

⋆ E-mail: lucien.lehmann@xlim.fr
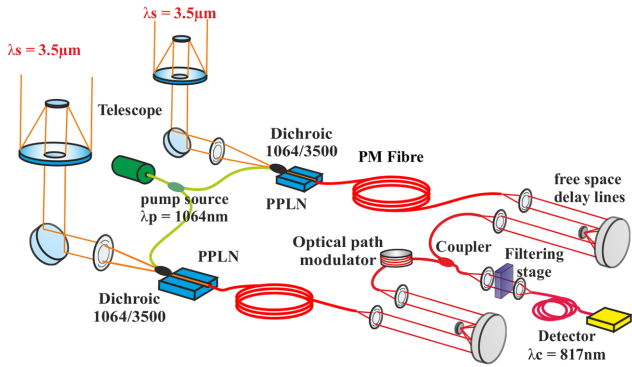
Figure 1. General principle of ALOHA. The optical fields collected by a set of telescopes are frequency shifted in non-linear crystals (Periodically Poled Lithium Niobate; PPLN) into the NIR bands. The beams are then transported using polarization-maintaining (PM) optical fibres and processed by guided components. After free space delay lines, the two converted beams are mixed in a fibre coupler and the fringe pattern is detected in the time domain by a silicon photon counting detector.

et al. 2017), here, we report on the practical on-sky sensitivity test using a single arm of the future ALOHA up-conversion interferometer at 3.5 μm. For this purpose, the signal optical field at frequency ν_s collected by the telescope is injected into a non-linear crystal powered by a strong monochromatic and coherent pump field at frequency ν_p. The converted wave at frequency $\nu_c = \nu_s + \nu_p$ is then created by sum-frequency generation (Boyd 2008). The set of frequencies ν_s, ν_p, ν_c have to satisfy the phase matching condition, which expresses that the converted field generated all along the non-linear crystal have to interact constructively with itself during its propagation. This condition induces a selection on the converted spectral bandwidth denoted the spectral acceptance of the non-linear crystal $\Delta\lambda$. This selectivity allows spectral multiplexing using a set of independent pump lasers around frequency ν_p (Lehmann et al. 2018b).

The goal of this study is to quantitatively investigate the up-conversion process, beam transport with spatial filtering and detection in a real observational situation. These tests took place at the coudé *f*/35 focus of the 1.04-m 'Epsilon' (East) telescope of the C2PU facility (Observatoire de la Côte d'Azur, Calern site, France; https://www.oca.eu/fr/c2pu-accueil).

2 EXPERIMENTAL SET-UP

This study focuses on sensitivity tests for a future MIR up-conversion interferometer at 3.5 μm. In this context, only a single interferometric arm is implemented as shown in Fig. 2, without any possibility of getting interferometric fringes.

The star light is collected by the 1.04-m telescope, then passes through the coudé optical train (seven mirrors, including the primary parabolic mirror, the secondary hyperbolic mirror and five flat bending mirrors) and finally is reflected by the tip-tilt mirror. The visible part of the beam is transmitted through the dichroic mirror D1 to a tip-tilt monitoring camera. The MIR part of the beam is reflected by D1 and time modulated at 140 Hz by a chopper to enhance the signal-to-noise ratio (SNR) of the converted signal. In the interferometric configuration, the chopper will be replaced by the signal modulation generated by the fringe pattern itself. The MIR beam is then launched into a ZBLAN (Poulain, Poulain & Lucas 1975) Fluoride Glass (ZFG) SM fibre at 3.5 μm by the off-axis parabola P1. The main purpose of this fibre is to fully decouple the
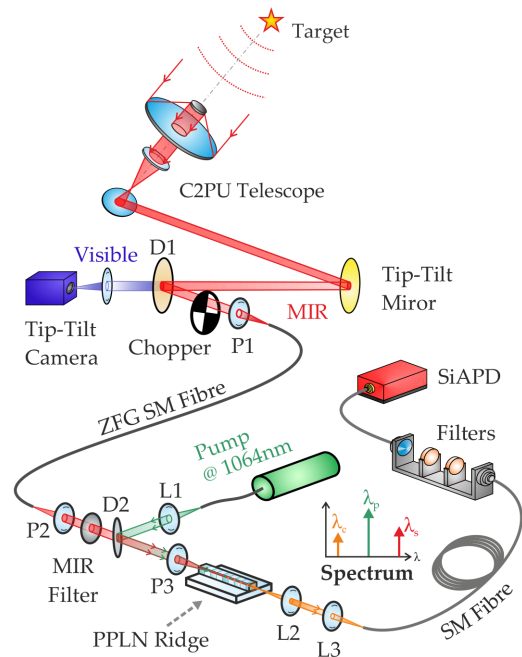
Figure 2. Simplified schematic of the experiment. D1,D2: dichroic mirror; P1, P2, P3: off-axis parabolas; L1, L2, L3: microscope objectives. The frequency conversion takes place in the non-linear PPLN ridge waveguide.

alignment of the light collecting stage with the frequency conversion and detection stages, thus significantly facilitating the instrument alignment. Moreover, the spatial filtering performed by the ZFG fibre allows us to calibrate our instrument and the transmission of the telescope with an internal thermal source. However, this fibre will not be necessary in the future interferometric configuration.

The non-linear optical component consists of a 20 mm long Periodically Poled Lithium Niobate (PPLN) waveguide using the ridge technology (Chauvet et al. 2016) with a poling period of $\Lambda = 19.9\,\mu m$ compliant with the quasi-phase matching for the working wavelengths. The MIR light is combined with 68 mW of pump laser at 1065 nm through the D2 dichroic mirror. Both are injected into the waveguide by the off-axis parabola P3. The maximum conversion efficiency is obtained at $\lambda_{s_0} = 3521$ nm ($\lambda_{c_0} = 817.7$ nm) and the spectral acceptance bandwidth is equal to $\Delta\lambda_s = 37$ nm, corresponding to a converted bandwidth $\Delta\lambda_c = 2$ nm around 817.7 nm.

The frequency conversion process requires that all the interacting waves (signal, pump, and converted) have the same linear polarization. Thus, all the guided components downstream the non-linear stage are SM and polarization maintaining at 818 nm for full compliance with the future interferometric configuration. Hence, all the following power values will be given for a single polarization, even if the source is randomly polarized.

The converted signal is collected by a 10 m SM optical fibre at 818 nm using a pair of microscope objectives. This fibre could have been hundreds of meters long without significant performance losses. At the fibre output, the converted signal is spectrally filtered by a set of interferometric filters to remove the pump residual. Finally, the converted signal is detected by a silicon avalanche photodiode (SiAPD) working in the photon counting regime.

In order to distinguish between the star signal and the intrinsic noise of our instrument, we temporally modulate the incoming star light using the optical chopper. However, all objects at room
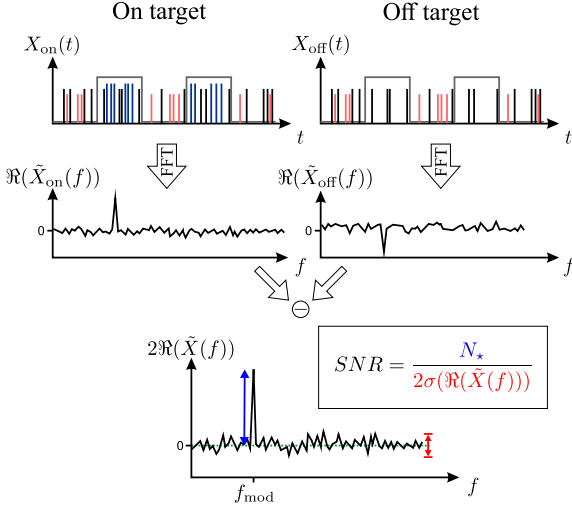
Figure 3. Data processing. On the frames X_{On} and X_{Off}, the square function shows the chopper position (1: passing, 0: blocking), the black lines are the dark count, the smaller red lines are the photoevents due to the chopper blades and the longer blue lines those due to the star.

temperature emit light in the MIR, including the chopper blades themselves. Therefore, to subtract the light emitted by the chopper blades from our measurements, we alternatively observe the star and a nearby patch of sky. This nodding also takes into account other spurious light sources, coming mainly from the sky background and the telescope itself.

3 DATA PROCESSING

Fig. 3 details the data processing performed on our measurements. The raw data are composed of two sets of frames: one with the telescope pointing to the target star (on-target) and the second pointing the sky background (off-target). Each frame is one second long and we average over 6 min of acquisitions before switching on or off target. We repeat this process a number of times depending on the magnitude of the star and the integration time. We call X_{On} and X_{Off}, respectively, the temporal acquisitions averaged over the total observation duration. X_{On} and X_{Off} are constituted by a modulated signal at the frequency of the chopper and a white noise B mainly caused by the dark count of the up-conversion detector. This dark count is due to the SiAPD itself and the parasitic non-linear optical effects (Pelc et al. 2010).

The modulated signal is comprised of four components $N_\star$, N_{BG}, N_{tel}, N_{chp}: the number of photoevents related to the star, the sky background, the telescope, and the chopper blades, respectively. By construction, the signal coming from the chopper blade surface is 180° phase shifted with respect to the three other ones. Therefore, if the acquisition is synchronized with the chopper, the real part of the Fourier transform of the on-target and of the off-target signal at the modulation frequency f_{mod} can be written as:

$$2\Re(\tilde{X}_{On}(f_{mod})) = N_\star + N_{BG} + N_{tel} - N_{chp} + \Re(B) \quad (1)$$

$$2\Re(\tilde{X}_{Off}(f_{mod})) = N_{BG} + N_{tel} - N_{chp} + \Re(B'). \quad (2)$$

B and B' are the complex values of the white noise at the frequency f_{mod} for each signal. The factor 2 takes into account the signal at the negative frequency of the Fourier transform.

Assuming that N_{BG}, N_{tel}, and N_{chp} slowly vary compared to the integration time, we can extract $N_\star$:

$$2\Re[\tilde{X}_{On}(f_{mod}) - \tilde{X}_{Off}(f_{mod})] = N_\star + \Re(B - B') = N_\star \pm \sigma. \quad (3)$$

$\Re(B - B')$ follows a Gaussian probability distribution with a null mean value and a standard deviation σ. In order to compare the signal $N_\star$ and the noise, we compute the following SNR:

$$\text{SNR} = \frac{N_\star}{\sigma} \approx \frac{N_\star}{2\sigma\left[\Re(\tilde{X}(f \gg f_{mod}))\right]}, \quad (4)$$

where $\tilde{X}(f) = \tilde{X}_{On}(f) - \tilde{X}_{Off}(f)$ and $\sigma\left[\Re(\tilde{X}(f \gg f_{mod}))\right]$ is the standard deviation of the real part of the Fourier Transform, away from the modulation peak and its harmonics. We use this value as an estimator of σ.

4 EXPERIMENTAL RESULTS

Table 1 summarizes the measurements performed during the night of 2018 June 9th–10th. We managed to detect stars from $L_{mag} = -3.12$ to $L_{mag} = 2.77$ with a spectral resolution close to $\lambda_s/\Delta\lambda_s = 100$ and SNR ranging from 232 to 2.7. Fig. 4 shows the differential real part of the Fourier transform as defined by equation (3) for each target. The modulation peak at 140 Hz is clearly visible for the four brightest stars. It is less apparent for HD 186882 (* δ Cyg), showing the sensitivity limit of the instrument.

All these measurements are dominated by the noise of the dark count of the instrument and the signal photon noise is negligible. Therefore the SNR evolves linearly with the flux of the star and as the square root of the integration time.

In order to calibrate our instrument, we used an internal source at $T_{int} = 60\,°C$ with a high emissivity coating (candle soot). The modulated power emitted by a blackbody on a single polarization writes:

$$P = \frac{1}{4} \times \Delta\lambda_s \times \Delta\Omega \times \Delta S \times \left[B(\lambda_s, T_{int}) - B(\lambda_s, T_{chp})\right], \quad (5)$$

where $\Delta\lambda_s$ is the bandwidth of the spectral acceptance of the non-linear waveguide, $\Delta\Omega$ the emission solid angle, ΔS the emission surface, T_{chp} the temperature of the chopper blades, and $B(\lambda, T)$ the spectral radiance of the blackbody. The internal source is placed before the ZFG fibre, which selects a single spatial mode, therefore $\Delta\Omega \times \Delta S = \lambda_s^2$. The factor four takes the selection of a single polarization and the duty cycle of the chopper into account.

The instrument received around 100 fW (1.7×10^6 photons per second) of modulated polarized flux from this internal source and we measured ≈1100 modulated converted photons per second. Hence, the quantum efficiency of the whole instrument is QE = 6.6×10^{-4}. This value takes into account all the losses between the ZFG fibre and the SiAPD detector as well as its quantum efficiency. We can use this value to calculate the noise equivalent power (NEP) of the instrument:

$$\text{NEP} = \frac{hc}{QE\lambda_s}\sqrt{2DC}. \quad (6)$$

With a dark count DC = 10 kHz, we got a NEP = 12 fW Hz$^{-1/2}$. This value is one order of magnitude better than commercially available single pixel detectors at these wavelengths (e.g. the PVI-4TE-4 by Vigo System has a NEP equal to 125 fW Hz$^{-1/2}$ for a 0.5×0.5 mm detector). The lack of spectral and spatial selectivity of this kind of detector explains their lower NEP despite a much higher quantum efficiency. An increase of the NEP by a factor of ten would reduce the limiting magnitude by 2.5.

Table 1. Results of the observation night from 2018 June 9th to 10th.

Source	Observation time	Airmass	L_{mag}	Flux[a] (fW nm^{-1})	(Jy)	Integration time (s) on target	off target	$N_\star$ (ph s^{-1})	SNR (σ)
HD 124897 ($\ast \alpha$ Boo)	22:51	1.12	−3.12	5100	955	60	0	4762	232
HD 164058 ($\ast \gamma$ Dra)	23:37	1.16	−1.44	1080	204	120	0	787	61.2
HD 172167 ($\ast \alpha$ Lyr)	03:25	1.01	0	288	54	180	180	250	15.4
HD 188947 ($\ast \eta$ Cyg)	04:00	1.03	1.53	70.4	13.4	720	900	46	5.99
HD 186882 ($\ast \delta$ Cyg)	04:39	1.01	2.77	22.5	4.2	720	1080	20	2.73
Sky background	05:07	1.01	–	–	–	0	180	−96[b]	8.31
Internal	05:41	–	–	18.2	–	180	0	1114	97.9

[a]Spectral flux density on a single polarization.
[b]Typical value for $N_{BG} + N_{tel} - N_{chp}$.
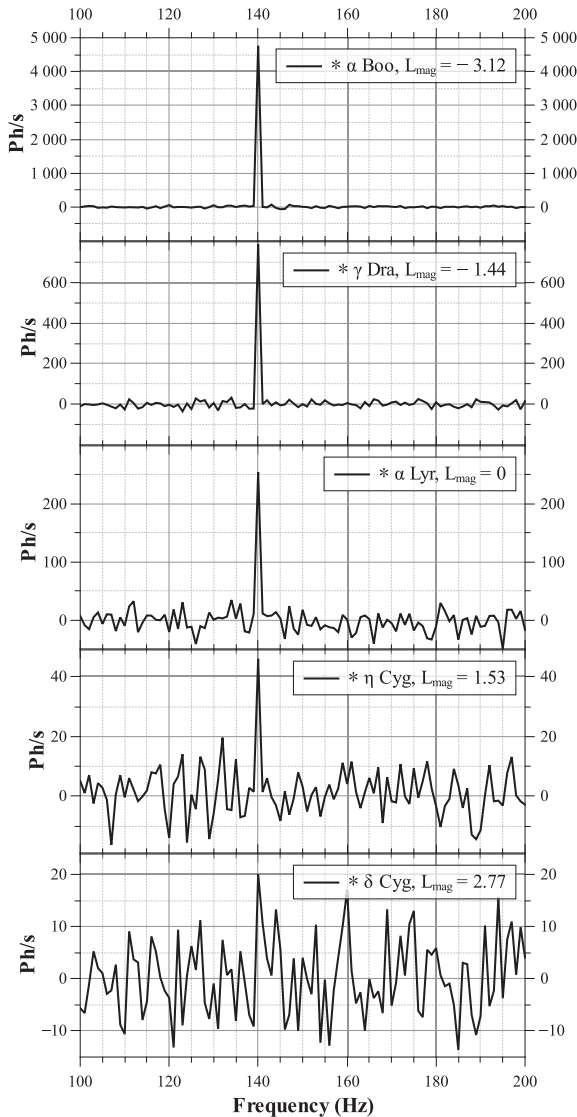
Figure 4. Final value of $2\Re(\tilde{X}(f))$ for the five observed stars.

The performance of the up-conversion instrument highly depends on the performance of the non-linear stage. The PPLN used is a first prototype and significant technological improvements are possible. For instance, in terms of transmission, it would be necessary to provide an antireflection coating at both ends of the waveguide, and a pigtailed PPLN (Umeki, Tadanaga & Asobe 2010) output would improve the coupling of the converted signal in the optical fibre.

By comparing the internal source with a star of similar brightness (HD 186882 ; $\ast$ del Cyg), we roughly estimate the transmission coefficient before the ZFG fibre (telescope, tip-tilt system, fibre injection) between 1 and 2 per cent. This throughput could be enhanced by reducing the number of mirrors of the optical train and using a dedicated mirror coating.

5 CONCLUSION

In this paper, we demonstrate the potential of ALOHA in the *L* band with an on-sky sensitivity test. Despite a low-coupling efficiency (about 1 per cent) between our instrument and the 1-m class telescope, and an unoptimized non-linear component, we managed to detect stars with magnitudes up to $L_{mag} = 2.8$, with a spectral resolution $\lambda_s/\Delta\lambda_s = 100$ and a total integration time up to 30 m. The current technological development of our instrument being far from its maximum potential, these preliminary results make us confident about the potential of the SFG interferometer as a new proposal for the MIR high-resolution imaging. This work is a significant step towards a possible implementation of ALOHA in the *L* band at the CHARA Array.

In the future, the conversion stage will be placed as close as possible to the telescope focus in order to increase the transmission and reduce the thermal background. After conversion the beam transport will be achieved through a silica fibre with the possibility to design very long baseline configurations.

REFERENCES

Boyd R. W., 2008, Nonlinear Optics, 3 edn. Academic Press, Amsterdam, Boston
Brummelaar T. A. t. et al., 2005, ApJ, 628, 453
Chauvet M., Henrot F., Bassignot F., Devaux F., Gauthier-Manuel L., Pêcheur V., Maillotte H., Dahmani B., 2016, J. Opt., 18, 085503
Darré P. et al., 2016, Phys. Rev. Lett., 117, 233902

Defrère D. et al., 2018, Exp. Astron., 46, 475

Delage L., Reynaud F., 2001, Opt. Express, 9, 267

Foresto V. C. d., 1994, in Roberson J. G., Tango W. J., eds, Proc. IAU Symp., Vol. 158, Very High Angular Resolution Imaging. Cambridge University Press, Cambridge, p. 261

Hinz P. M. et al., 2016in Malbet F., Creech-Eakman M. J., Tuthill P. G., eds, SPIE Conf. Ser., Vol. 9907. Optical and Infrared Interferometry and Imaging V. SPIE, Bellingham, p. 990714

Lawson P. R., 1997, Selected Papers on Long Baseline Stellar Interferometry. SPIE Optical Engineering Press, Bellingham

Lehmann L. et al., 2018a, Exp. Astron., 46, 447

Lehmann L., Darré P., Boulogne H., Delage L., Grossard L., Reynaud F., 2018b, MNRAS, 477, 190

Lopez B. et al., 2014, The Messenger, 157, 5

Mennesson B. et al., 1999, A&A, 346, 181

Monnier J. D. et al., 2018, Exp. Astron., 46, 517

Pelc J. S., Langrock C., Zhang Q., Fejer M. M., 2010, Opt. Lett., 35, 2804

Petrov R. G. et al., 2007, A&A, 464, 1

Poulain M., Poulain M., Lucas J., 1975, Mater. Res. Bull., 10, 243

Szemendera L., Grossard L., Delage L., Reynaud F., 2017, MNRAS, 468, 3484

Umeki T., Tadanaga O., Asobe M., 2010, IEEE J. Quantum Electron., 46, 1206

This paper has been typeset from a TEX/LATEX file prepared by the author.